ELectronics EXpress

IEICE Electronics Express, Vol.7, No.20, 1539–1545

A maximum power point tracking circuit of thermoelectric generators without digital controllers

Shiho Kim[a)], **Sungkyu Cho, Namjae Kim, and Jungyong Park**

Dept. of Electrical Engineering, Chungbuk National University, Chungbuk, 361–763, Korea

a) *shiho@chungbuk.ac.kr*

Abstract: A digital coreless maximum power point tracking (MPPT) circuit for thermoelectric generator unit is proposed and fabricated. The experimental and simulation results from the proposed MPPT circuit dealt with rapid variation of temperature and abrupt changes of load current have shown that the proposed method allows stable operation with high power transfer efficiency. The proposed MPPT circuit has a merit in cost and miniaturization of a system compared to conventional MPPT algorithms thanks to an analog tracking circuit without digital controller unit for calculating peak power point by iterative methods.

Keywords: maximum power point tracking, MPPT, thermoelectric generators

Classification: Integrated circuits

References

[1] R. Kim and J. Lai, "A Seamless Mode Transfer Maximum Power Tracking Controller For Thermoelectric Generator Applications," *IEEE Trans. Power Electron.*, vol. 23, no. 5, Sept. 2008.

[2] R. Kim, J. Lai, B. York, and A. Koran, "Analysis and Design of Maximum Power Point Tracking Scheme for Thermoelectric Battery Energy Storage System," *IEEE Trans. Ind. Electron.*, vol. 56, no. 9, pp. 3709–3716, 2009.

[3] D. Mitrani, A. Tome, J. Salazar, A. Turo, M. Garcia, and J. Charvez, "Methodology for Extracting thermoelectric module parameters," *IEEE Trans. Instrum. Meas.*, vol. 54, no. 4, pp. 1548–1552, 2005.

[4] N. Kasa, T. Iida, and L. Chen, "Flyback inverter controlled by sensorless current MPPT for photovoltaic power system," *IEEE Trans. Power Electron.*, vol. 52, no. 4, pp. 1145–1152, July 2005.

[5] N. Femia, G. Petrone, G. Spagnuolo, and M. Vitelli, "Optimization of perturb and observe maximum power point tracking method," *IEEE Trans. Power Electron.*, vol. 20, no. 4, pp. 963–973, July 2005.

[6] T. Kottas, Y. Boutalis, and A. Karlis, "New maximum power point tracker for PV arrays using fuzzy controller in close cooperation with fuzzy cognitive networks," *IEEE Trans. Energy Convers.*, vol. 21, no. 3, pp. 793–803, 2006.

DOI: 10.1587/elex.7.1539
Received August 20, 2010
Accepted September 28, 2010
Published October 25, 2010

[7] H. Nagayoshi, K. Tokumisu, and T. Kajikawa, "Evaluation of multi MPPT thermoelectric generator system," *International Conference on Thermoelectrics*, pp. 318–321, 2007.
[8] I. Laird, H. Lovatt, N. Savvides, D. Lu, and V. G. Agelidis, "Comparative Study of Maximum Power Point Tracking Algorithms for Thermoelectric generators," *Australasian Universities Power Engineering Conference*, pp. 1–6, 2008.

1 Introduction

There has been a great interest in development of renewable green energy technologies, due to depletion of fossil energy sources and the environmental issues regarding reduction of green house gas emission. Thermoelectric generator (TEG) is a solid state semiconductor device which converts temperature difference between hot and cold sides into electrical energy [1, 2, 3]. To maximize energy conversion efficiency, maximum power point tracking (MPPT) scheme should be implemented. For the MPPT methods, there have been significant researches in photovoltaic applications. Even though many MPPT algorithms such as the perturbation and observation methods, the incremental conductance methods, or the ripple correlation control methods, fuzzy logic and a neural network based model have been successfully used in photovoltaic applications [4, 5, 6], these methods are not optimized to the power-versus-current characteristics of TEG. Recently, a practical MPPT conditioner to reduce mismatch power loss and improve load matching ability of TEG system has been developed [7]. Moreover, a new technology with a seamless mode transfer MPPT [1] and MPPT scheme with thermoelectric battery storage system [2] have proposed for vehicular battery charging applications of TEG. However, these methods still require a microcontroller unit to calculate peak power point by iterative methods, so it is not appropriate TEG applications requiring low cost of implementation as well as high power conversion efficiency. In this paper, an analog MPPT algorithm and circuit for TEG with constant voltage mode are proposed and experimentally tested.

2 Characteristics of Thermoelectric Generators and Proposed MPPT Controller

TEG can be modeled as a voltage source of V_{OC} having internal resistance of R_S which can be extracted by V_{OC}/I_{SC} [3]. Where, V_{OC} is an open circuit voltage proportional to temperature difference (ΔT) and Seebeck coefficient (S), and I_{SC} is short circuit current. Since power is a product of terminal voltage (V_{tem}) and output current (I_{tem}), output power P can be expressed as,

$$P = I_{tem}V_{tem} = \left(\frac{V_{tem}(V_{OC} - V_{tem})}{R_S}\right) \quad (1)$$

Therefore, we can get terminal voltage at the maximum power point at

DOI: 10.1587/elex.7.1539
Received August 20, 2010
Accepted September 28, 2010
Published October 25, 2010

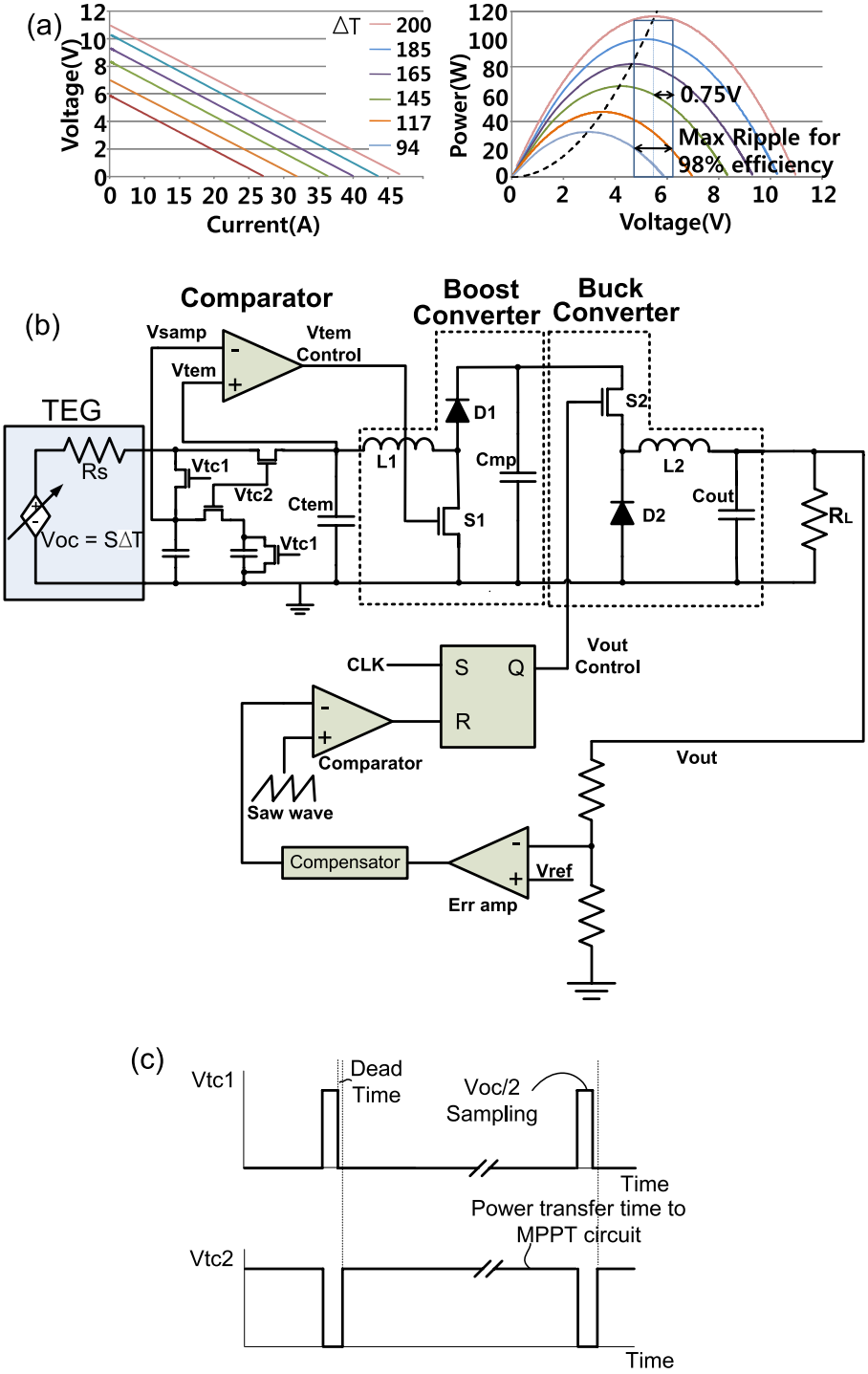

Fig. 1. (a) Measured voltage versus-current characteristics and Power versus voltage characteristics of a Bi2Te3 thermoelectric module. (b) Proposed MPPT circuit employing the boost cascaded-with-buck converter with feedback circuit for constant output voltage. (c) Waveforms of V_{tc1} and V_{tc2} sample and hold timing signal

DOI: 10.1587/elex.7.1539
Received August 20, 2010
Accepted September 28, 2010
Published October 25, 2010

the half of the open circuit voltage, and corresponding ideal maximum output power, P_{max}, as following equations [1, 7];

$$V_{tem}|_{\max} = \frac{V_{OC}}{2}, \; and \, P_{\max} = \frac{{V_{OC}}^2}{4R_S} = \frac{(R_S I_{SC})^2}{4} \tag{2}$$

Fig. 1(a) shows measured voltage versus current and corresponding power versus voltage characteristics of a Bi2Te3 thermoelectric module. Here, the dashed line shows Maximum power points located at the half of VOC. Fig. 1(b) shows proposed MPPT circuit employing the boost cascaded-with-buck converter with a feedback circuit for DC output voltage of buck converter. Proposed MPPT circuit consists of V_{OC} sampling and timing control circuitry, comparator and DC-to-DC converter with feedback circuit. The sampling part samples and holds the half of V_{OC} values periodically, where V_{tc1} and V_{tc2} shown in Fig. 1(c) are signals for sample and hold timing control. The Comparator compares terminal voltage (V_{tem}) with sampling voltage (V_{samp}) and produces a control signal to the DC-to-DC converter part. When V_{tc1} is high and V_{tc2} is low, V_{OC} value is sampled. On the other hand, during V_{tc1} is low and V_{tc2} is high, the sampling circuit holds half of V_{OC} value. The dead time shown in Fig. 1(c) is a margin to avoid overlap between V_{tc1} and V_{tc2}. The sample frequency should be decided by a temperature changing rate of TEG. In the vehiclar application, a sampling frequency about 2 Hz is fast enough by assuming the rate of temperature variation of thermoelectric modules is lower than 1°C per second. Since the Seebeck coefficient of widely used thermoelectric materials is less than several hundreds μV/Kelvin, we can presume that a variation of V_{OC} value during 0.5 second causes negligible shift in maximum power point. The boost converter in the DC-to-DC converter part is controlled by output signal of the comparator, whereas output voltage of a load resistor (R_L) is regulated by buck converter thanks to a feedback circuit shown in Fig. 1(b). During V_{samp} is lower than V_{tem}, the high state of comparator-out makes the switch S1 close, resulting in an increase in the inductor current which is same as the output current from TEG (I_{tem}). As a consequence of increase in I_{tem}, the terminal voltage V_{tem} drops propotional to the amount of I_{tem} and the internal resistance R_S. Eventually V_{tem} becomes lower than level of $V_{OC}/2$, then low state of comparator output turns off the switch S1, and inductor current path is through the flyback diode D1. Since inductor current is decreased while S1 is open, the terminal voltage V_{tem} rise toward level higher than $V_{OC}/2$, then S1 is close again. A feedback loop consists of TEG, comparator and boost converter works like a bistable multivibrator generating a sequence of pulse width modulated signal. The frequency of the pulse depend on the effective RC delay time constant of the feedback loop.

3 Simulation Results

Fig. 2 shows SPICE simulated voltage waveforms of the proposed MPPT circuit with the boost-cascaded-with-buck converter. The sampling frequency

DOI: 10.1587/elex.7.1539
Received August 20, 2010
Accepted September 28, 2010
Published October 25, 2010

of V_{tc1} and V_{tc2} was set to 2.4 Hz with sampling duration of 1 μsec, and control pulse of the Buck converter was 100 KHz. We use an electrical model of TEG extracted from measured data shown in Fig. 1, employing a voltage source $V_{OC} = S\Delta T$ with internal resistance R_S of 0.26 Ω for SPICE simulations. Simulation result shows that voltage level of V_{tem} is tracking the half value of V_{OC} with a maximum ripple voltage of 0.6 V while V_{OC} changes from 11 V to 6 V with a changing rate of 1 V/sec. The voltage change rate of 1 V/sec is corresponding to temperature change rate of 20°C/sec in the measured data shown in Fig. 1(a), so that it is a more than enough estimation of temperature variation in vehicular applications. The output voltage is set to 12.8 V which is a typical charging voltage level of lead-acid battery. It takes about 4 seconds during V_{out} is rising from initial 0 V to steady state level of

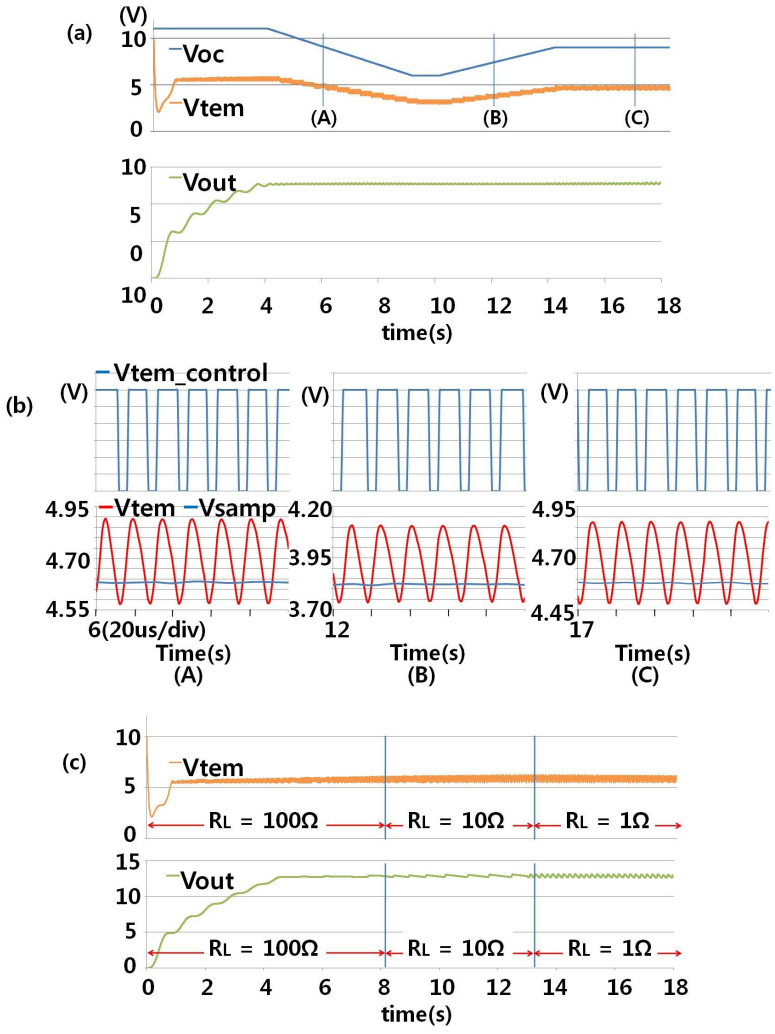

Fig. 2. (a) SPICE simulated voltage waveforms of the proposed MPPT circuit with load resistance of 5 W. (b) Voltage of comparator output (Vtem_control), Vsamp, and Vtem at the timing of (A), (B), and (C). (c) Simulated voltage waveform of V_{out}, V_{tem} and V_{samp} against abrupt change of R_L while V_{OC} is fixed at 11 V.

DOI: 10.1587/elex.7.1539
Received August 20, 2010
Accepted September 28, 2010
Published October 25, 2010

12.8 V.

Fig. 2(b) shows simulated output pulse of the comparator (signal named as $V_{tem\_control}$), V_{samp}, and V_{tem} at the point of (A), (B), and (C) marked on Fig. 2(a). The frequency of the comparator output pulse is about 70 KHz. The frequency depends on the effective RC time delay of the feedback loop composed of TEG, comparator and boost converter. Since Ctem was 10 μF, and RC delay time is about 14.3 μsec, the effective resistance value of the loop is about 1.43 Ω.

The power transfer efficiency was larger than 98% in all cases of decreasing, ascending or stable condition of V_{OC}. The power transfer efficiency was calculated ratio between theoretical maximum power given by Eq. (2) and simulated power obtained by following Eq. of $V_{tem} \times I_{tem}$.

Fig. 2(c) shows SPICE simulated voltage waveform as a response against abrupt change of R_L while V_{OC} is fixed at 11 V. The voltage level of V_{out} and V_{tem} remains almost unchanged regardless of abrupt change of R_L for two orders of magnitude from 100 to 1 Ω. However, ripple voltage of V_{out} and V_{tem} is increased when R_L becomes smaller, because the output voltage is remaining at DC level of 12.8 V so that output current is inversely proportional to R_L. The ripple voltage in V_{out} is mainly caused by the output capacitance and output current level of the buck converter and feedback circuit shown in Fig. 1(b). Larger output current causes corresponding higher ripple voltage in DC-to-DC buck converters. The simulated peak ripple voltage of V_{tem} is about 0.38 V and 0.62 V, when R_L is 100 and 1, respectively.

4 Experimental results and Discussions

A test chip was designed and fabricated by using a 0.5-μm CMOS process. The chip includes timing control, sampling, comparator, and feedback circuit for buck converter, etc. Fig. 3 shows measured voltage of comparator output, V_{samp}, V_{tem} and V_{out} for the condition of $V_{OC} = 7$ V, $R_S = 5\,\Omega$, and Ctem = 10 μF. The measured frequency of comparator output is 340 Khz with duty of 0.63, and ripple of V_{tem} is 0.7 V, respectively. The power transfer efficiency at the max power point is closely related to the amplitude of ripple voltage. A relationship between V_{tem} ripple voltage and output power is represented in Fig. 1(a), for the case of V_{OC} is equal to 11 V curve. The power transfer efficiency is higher than 98% in Fig. 1(a), unless the ripple voltage is lower than 0.75 V.

There are two feedback loops in proposed MPPT circuit. One front-end feedback loop consists of TEG, sampling circuit, comparator and boost converter, and another is back-end output voltage feedback loop of the buck converter. Since the front-end loop works like a bi-stable multi-vibrator generating a sequence of pulse width modulated signal, it is clear that stability depends on the back-end loop of the buck converter circuit. If we design an output voltage feedback loop of the buck converter with sufficient phase margin, we can avoid the stability issue of the MPPT circuit.

In the comparative study of MPPT algorithms for thermoelectric gener-

DOI: 10.1587/elex.7.1539
Received August 20, 2010
Accepted September 28, 2010
Published October 25, 2010

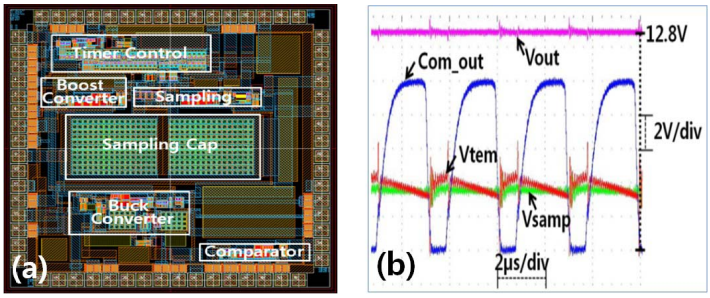

Fig. 3. (a) Layout view of the fabricated Chip with area of 3 mm × 3 mm (b) Measured voltage waveforms of the V_{out}, comparator output. V_{samp}, and V_{tem}

ators, power transfer efficiency of conventional P&O method and Incremental Conductance method is from 88 to 94% [8]. Where, Power consumption caused by micro controller units was not considered in the comparative study [8]. Conventional methods of MPPT algorithms require DSP or micro controller units for calculating peak power point by iterative methods. Demerits of conventional methods of MPPT algorithms are cost of implementation as well as power loss by operating power of micro controller units. Advantage of proposed circuit is tracking the maximum power point by analog tracking circuit sampling half V_{OC} level without DSP or micro controller unit.

5 Conclusions

A maximum power point tracking circuit for thermoelectric generators without digital controller unit was proposed. Advantage of proposed method is analog tracking circuit by sampling half V_{OC} level without DSP or micro controller unit for calculating peak power point by iterative methods. The simulation results dealt with rapid variation of temperature and abrupt changes of load current have shown that the proposed method allows stable operation with high power transfer efficiency. The proposed MPPT circuit has an advantage in implementation cost, miniaturization, and power conversion efficiency compared to the conventional MPPT algorithms.

Acknowledgments

The Authors thank to IDEC for supporting EDA tools and MPW shuttle service. This work was supported by the MKE, Korea, under the ITRC support program supervised by the NIPA (NIPA-2009-C1090-0904-0007).

DOI: 10.1587/elex.7.1539
Received August 20, 2010
Accepted September 28, 2010
Published October 25, 2010